Journal of
Plankton Research

plankt.oxfordjournals.org

Featured Article

J. Plankton Res. (2015) 37(5): 869–885. First published online August 6, 2015 doi:10.1093/plankt/fbv062

Modelling alkaline phosphatase activity in microalgae under orthophosphate limitation: the case of *Phaeocystis globosa*

CAROLINE GHYOOT[1]*, NATHALIE GYPENS[1], KEVIN J. FLYNN[2] AND CHRISTIANE LANCELOT[1]

[1]UNIVERSITÉ LIBRE DE BRUXELLES, ECOLOGIE DES SYSTÈMES AQUATIQUES, CP-221, BOULEVARD DU TRIOMPHE, 1050 BRUSSELS, BELGIUM AND
[2]CENTRE OF SUSTAINABLE AQUATIC RESEARCH, SWANSEA UNIVERSITY, SWANSEA SA2 8PP, UK

*CORRESPONDING AUTHOR: cghyoot@ulb.ac.be

Received January 13, 2015; accepted July 12, 2015

Corresponding editor: Pia Moisander

Many phytoplankton exploit phosphorus (P) from organic sources when dissolved inorganic P (DIP) is depleted. This process is, however, rarely considered in ecological and biogeochemical models. We present a mechanistic model describing explicitly the ability of phytoplankton to use dissolved organic P (DOP) when DIP is limiting, by synthesizing alkaline phosphatase (AP) that releases DIP from DOP. This model, applicable to any phytoplankton species expressing AP, is here specifically developed for the colony-forming *Phaeocystis globosa*. It describes the main processes related to P metabolism, including DIP transport, intracellular accumulation and assimilation. Model behaviour is explored in DIP-limiting batch-type conditions for different DOP ranging between 0 and 1.5 mmol P m^{-3}. Simulations show that the DOP-derived DIP increases the maximum biomass reached and extends the period of net growth. The magnitude of the enhanced biomass production is controlled by the DOP initially present as well as the released DOP, the latter being recycled by lysis of *P. globosa* cells. We also present a simplified model version derived from the mechanistic model, which involves fewer state variables and parameters. The latter is directly usable in both variable (quota-type) and fixed stoichiometry descriptions of phytoplankton growth.

KEYWORDS: P limitation; alkaline phosphatase activity; modelling; *Phaeocystis globosa*

INTRODUCTION

Phosphorus (P) is fundamental to all life processes and is therefore an essential element for growth. The preferred source of P for phytoplankton is dissolved inorganic P (DIP) (Cembella *et al.*, 1984). In the absence of sufficient DIP, various metabolic processes are de-repressed to enable a more efficient use of internal P and/or to allow acquisition of P from organic sources (Gobler *et al.*,

2011; Wurch *et al.*, 2011; Dyhrman *et al.*, 2012). These processes include the increased ability to transport DIP (by increasing transporters affinity and/or the number of transporters), the lowering of P demand (by switching sulfolipids for phospholipids), the maximization of P recycling within the cell (by adjustment of the glycolysis pathway) and the up-regulation of ecto-proteins involved in P cleavage (phosphohydrolytic enzymes). Many freshwater and marine phytoplankton species have been shown to up-regulate the latter mechanism to satisfy their P needs from the dissolved organic P (DOP) under DIP limitation (Kuenzler and Perras, 1965; Cembella *et al.*, 1984; Flynn *et al.*, 1986; Hoppe, 2003; Glibert and Legrand, 2006). Different types of phosphohydrolitic enzymes can be expressed (such as alkaline and acid phosphatases, 5′ nucleotidase and phosphodiesterase) but emphasis is typically (and pragmatically for ease of measurement) placed only on the alkaline phosphatase (AP). As a wide variety of DOP can be exploited (van Boekel, 1991; Yamaguchi *et al.*, 2014), this strategy has important implications for the competitive success of phytoplankton in low DIP environments and for the related biogeochemical cycles. The ability to acquire P from different sources, including consumption of bacterial-P by mixotrophic phytoplankton (Mitra *et al.*, 2014) can be particularly important in oligotrophic ecosystems (Mather *et al.*, 2008) as well as in eutrophic waters (Rousseau *et al.*, 2004) frequently subjected to nutrient imbalance.

Despite the importance of AP for aquatic microbes and the competitive advantage that it can confer in low DIP environments, only few models explicitly consider the utilization of the DOP by phytoplankton as a P source under DIP limitation (e.g. Letscher and Moore, 2015). Some authors suggest that their phytoplankton models take the effect of AP into account, but they always do so implicitly. One way is to attribute a low half-saturation constant for DIP assimilation (e.g. Lancelot *et al.*, 2005). Another is to consider the expression of AP as a higher allocation in the P uptake machinery under P limitation with the effect of increasing the P maximum uptake rate (Klausmeier *et al.*, 2007; Pahlow and Oschlies, 2009; Bonachela *et al.*, 2013; Lomas *et al.*, 2014). However, all these models lack an explicit description of the development and expression of AP activity (APA) and do not consider the DOP actually available.

As a first step in explicitly including the ability of phytoplankton to use DOP, this work proposes a simple model formulation that can be easily included in large ecological and biogeochemical models. The simple formulation (hereafter referred to as M2) was derived from the analysis of results obtained from operating a mechanistic ordinary differential equations (ODE) model (hereafter referred to as M1) also detailed in this work. M1 describes explicitly the physiological mechanisms involved in up-regulation and expression of AP under conditions of P-stress caused by DIP limitation. Both M1 and M2 are applicable to all phytoplankton species expressing AP by the fact that the physiological mechanisms described here are not species-specific. However, the models were developed making use of *Phaeocystis globosa* as a model species for the choice of the parameter values. This haptophyte often grows in large ungrazable colonies composed of cells embedded in a mucilaginous matrix, and is responsible for large ecosystem disruptive bloom events in eutrophied seas such as the Southern North Sea (Lancelot *et al.*, 1987; Lancelot, 1995). This species has been previously shown to synthesize AP when ambient DIP is low (Veldhuis and Admiraal, 1987; Veldhuis *et al.*, 1987; van Boekel and Veldhuis, 1990) and is suspected to acquire DIP from DOP hydrolysis to help sustain massive spring blooms in nitrate-enriched waters such as the Southern North Sea. This particular eutrophied coastal system now displays symptoms of DIP limitation due to nutrient (pollution) control measures implemented in the late 1980s that were more successful in decreasing P inputs rather than N inputs (Rousseau *et al.*, 2004; Billen *et al.*, 2005; van der Zee and Chou, 2005; Passy *et al.*, 2013).

In the absence of suitable published batch experimental data, M1 was constructed and tested to match the available qualitative observations related to phosphate transport, intracellular accumulation and AP induction/activity reported for *P. globosa* or for another haptophyte such as *Emiliania huxleyi* (Table I). The performance of M2, in which APA is implicitly considered to properly describe phytoplankton and nutrient dynamics under DIP depletion and DOP availability was then appraised by comparison with the results obtained with M1 taken as "reference." Finally, the mechanistic model M1 was used to explore (i) the extent to which APA can sustain phytoplankton growth under DIP depletion and (ii) the effect of different capacity to accumulate internal P reserves. These two aspects are indeed of major interest when dealing with competition between species in DIP-limiting environments.

METHOD

Model description and parameterization

The mechanistic model (M1)

The structure of the mechanistic model built for *P. globosa* colonies is schematically shown in Fig. 1A. This model is based on the AQUAPHY model (Lancelot *et al.*, 1991) describing carbon and nutrient flows within a strictly phototrophic phytoplankton cell, taking consideration of the uncoupling between photosynthesis and growth. The

Table I: Qualitative observations related to phosphate transport, accumulation and alkaline phosphatase activity (APA) reported for P. globosa *or, if not available, for the haptophyte* E. huxleyi. *curves were sketched from data given in the jointed references*

Observations		Species	References
Phosphate transport			
(i) The maximum specific DIP uptake rate is regulated by the internal P content.	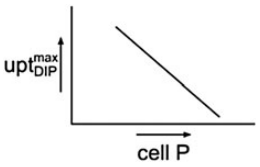	*E. huxleyi*	Riegman *et al.* (2000)
Phosphate storage			
(ii) Only a modest amount of P accumulation is observed in the presence of excess P (for *P. globosa* only two cells division are allowed with the accumulated P)		*Phaeocystis* sp., *E. huxleyi*	Jahnke (1989), Riegman et al. (2000), Shaked *et al.* (2006)
(iii) Under DIP depletion, colony and single cells both decrease their cellular P content	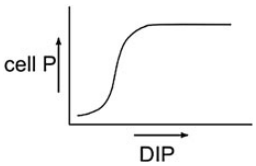	*P. globosa*	Veldhuis and Admiraal (1987)
(iv) DIP can be absorbed and accumulated in the colonial structure		*P. globosa*	Veldhuis *et al.* (1991)
Alkaline phosphatase activity			
(v) Under DIP depletion colony and single cells have high APA	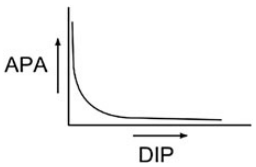	*P. globosa*	Veldhuis and Admiraal (1987)
(vi) AP synthesis occurs at the transition between the late exponential phase and the early stationary phase when the DIP concentration is very low	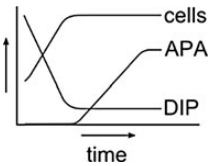	*E. huxleyi*	Kuenzler and Perras (1965), Dyhrman and Palenik (2003), Xu *et al.* (2010)
(vii) AP responds rapidly to fluctuations in P level in the environment	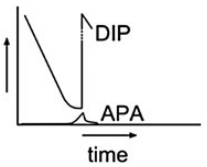	*E. huxleyi*	Dyhrman and Palenik (2003), Xu *et al.* (2006)
(viii) AP synthesis is regulated by an internal pool that is directly influenced by the influx of DIP into the cell		*P. globosa*	van Boekel (1991), Xu *et al.* (2006)
(xi) AP enzymes are rapidly lost when DIP is added back to P-stressed cultures	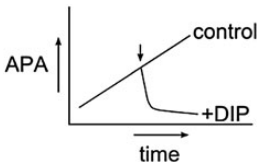	*E. huxleyi*	Dyhrman and Palenik (2003), Xu *et al.* (2006)

original AQUAPHY is here modified to explicitly describe the synthesis and the phosphohydrolytic activity of AP (grey rectangle in Fig. 1A). The model structure includes 12 state variables (Table II) linked by 19 processes (Supplementary data, Appendix A and B). State variables describing *P. globosa* physiology include: the functional and structural metabolites (F) with the exception of the AP that is described by a separate state variable, carbon monomers (early products of photosynthesis; S_C), internal carbon reserves (i.e. carbohydrate, fatty acids; R_C), intracellular soluble phosphate (S_P), polyphosphate reserves (R_P) and the extracellular mucus (M) in which colonial *P. globosa* cells are embedded and that provides an extracellular supplementary carbon reserve (Lancelot and Mathot, 1985).

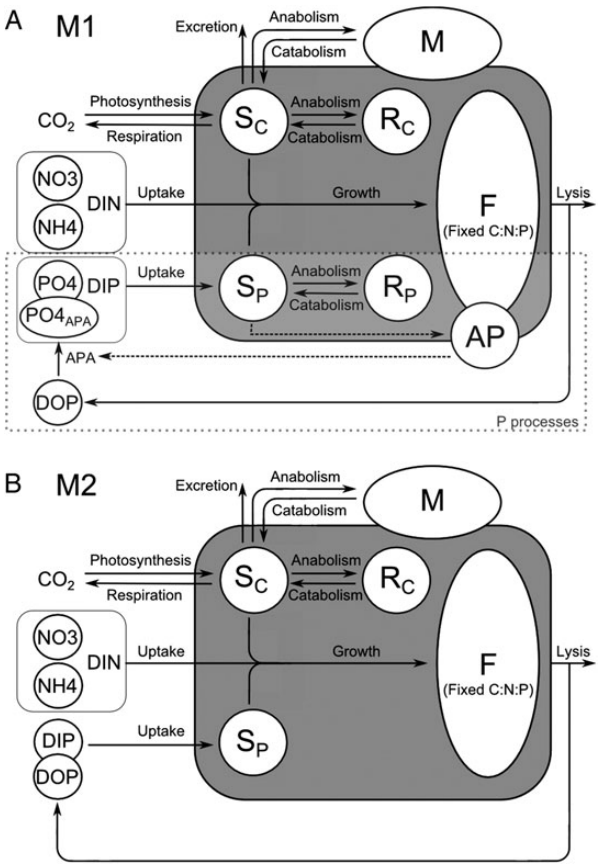

Fig. 1. Two alternative schemes for modelling the functioning of *P. globosa* colonies and their ability to use DOP to sustain growth when DIP is limiting. (**A**) Mechanistic model (M1) including five carbon pools: structural and functional metabolites (F), alkaline phosphatase (AP), carbon monomers (S_C), carbon reserves (R_C) and mucus (M), and two pools containing inorganic P: internal soluble phosphate (S_P) and polyphosphates (R_P). External nutrients include: dissolved inorganic nitrogen (DIN = NO_3 + NH_4), dissolved inorganic P (DIP = PO_4 + PO_{4APA}) and dissolved organic P (DOP). (**B**) Simplified model (M2) without R_P, AP and PO_{4APA}.

The total C-cell biomass (mmol C m^{-3}) of *P. globosa* is given by the sum of F, AP, S_C and R_C. The F pool is assumed to have a fixed C:N:P stoichiometry (Supplementary data, Appendix C) based on biochemical constraints in agreement with Geider and Laroche (Geider and Laroche, 2002). Similarly, AP has a fixed C:N stoichiometry (assumed to be the same as for the F pool). Variable cellular stoichiometry is enabled by taking account of the additional C and P accumulated as carbon monomers (S_C), carbohydrates and fatty acids (R_C), soluble inorganic phosphorus (S_P) and polyphosphates (R_P). Therefore, the C-biomass-based P-quota (PC) can be calculated as the ratio between P included in the F, S_P and R_P pools and C included in the F, AP, S_C and R_C pools. External nutrients involve: the nitrate (NO_3) and the ammonium (NH_4) that constitute the dissolved inorganic nitrogen pool (DIN), the ambient orthophosphate (PO_4) plus the newly formed orthophosphate released as a function of AP activity upon DOP (PO_{4APA}) that together constitute the DIP pool and finally the DOP. Processes that have been added or modified from the original AQUAPHY are described by the equations reported in Table III.

Synthesis of new metabolites F [growth in Fig. 1A; μ in Equation (1) of Table III] is controlled by the availability of carbon monomers S_C (either directly produced by photosynthesis or indirectly by R_C and M catabolism) and inorganic nutrients. The S_C limitation is described by a Michaelis–Menten equation where the substrate concentration is expressed by $X_{S_C} - k_{S_C}$ in which $X_{S_C} = S_C/F$ and k_{S_C} is the minimum value for X_{S_C} and is assumed to be equal to the half-saturation constant for S_C assimilation (Supplementary data, Appendix C). Simultaneous limitation by several nutrients is handled by invoking Liebig's minimum law in which P limitation is formulated by a hyperbolic function depending on X_{S_P}

Table II: State variables (all expressed as a concentration in seawater)

State variable	Description	Units
P. globosa (i = colony or single cells)		
F^i	Functional and structural metabolites	mmol C m^{-3}
AP^i	Alkaline phosphatase	mmol C m^{-3}
S^i_C	Carbon monomers (early products of photosynthesis)	mmol C m^{-3}
R^i_C	Intracellular carbon reserves (carbohydrates, fatty acids)	mmol C m^{-3}
S^i_P	Intracellular soluble phosphate	mmol P m^{-3}
R^i_P	Intracellular polyphosphate reserves	mmol P m^{-3}
M	Extracellular mucus (surrounding colony cells)	mmol C m^{-3}
External nutrients		
NO_3	Nitrate	mmol N m^{-3}
NH_4	Ammonium	mmol N m^{-3}
PO_4	Orthophosphate	mmol P m^{-3}
PO_{4APA}	Newly released orthophosphate from DOP	mmol P m^{-3}
DOP	Dissolved organic phosphorus	mmol P m^{-3}

Phaeocystis globosa biomass (colony + single cells) is given by $[F + S_C + R_C + AP]^{col} + [F + S_C + R_C + AP]^{sng}$ (mmol C m^{-3}).

Table III: Equations describing the processes that have been added or adapted compared with AQUAPHY for a better consideration of the phytoplankton P metabolism

Equation	Process	Value	Units	Explanation
1	μ	$\mu^{max} \times \frac{X_{S_C} - k_{S_C}}{(X_{S_C} - k_{S_C}) + k_{S_C}} \times \min\left[\frac{DIN}{DIN + k_N}, \frac{X_{S_P}}{X_{S_P} + k_{S_P}}\right] \times F$	mmol C m^{-3} h^{-1}	Synthesis of new metabolites F as a function of X_{S_C} (=S_C/F) and inorganic nutrients, i.e. DIN or X_{S_P} (=S_P/(F/CP_F))
2	s_{AP}	$s_{AP}^{max} \times \frac{X_{S_C} - k_{S_C}}{(X_{S_C} - k_{S_C}) + k_{S_C}} \times \frac{DIN}{DIN + k_N} \times \frac{(1 - X_{S_P}/X_{S_P}^{max})^{h_{s_{AP}}}}{(1 - X_{S_P}/X_{S_P}^{max})^{h_{s_{AP}}} + k_{S_{AP}}^{reg}} \times F$	mmol C m^{-3} h^{-1}	AP synthesis as a function of S_C and DIN and restricted by $X_{S_P}^{max}$
3	deg_{AP}	$k_{deg_{AP}} \times AP$	mmol C m^{-3} h^{-1}	Constant AP degradation
4	resp	$k_{maint} \times F + \xi \times (\mu + s_{AP})$	mmol C m^{-3} h^{-1}	Respiration
5	upt_{DIP}	$upt_P^{max} \times \frac{DIP}{DIP + k_P} \times \frac{(1 - X_{S_P}/X_{S_P}^{max})^4}{(1 - X_{S_P}/X_{S_P}^{max})^4 + k_{upt_P}^{reg}} \times \frac{F}{CP_F}$	mmol P m^{-3} h^{-1}	DIP (PO_4 + PO_{4APA}) uptake as a function of DIP and restricted by X_{S_P}
6	s_{R_P}	$s_{R_P}^{max} \times \frac{(X_{S_P}/X_{S_P}^{max})^4}{(X_{S_P}/X_{S_P}^{max})^4 + k_{s_{R_{P1}}}^{reg}} \times \frac{(1 - X_{R_P}/X_{R_P}^{max})^4}{(1 - X_{R_P}/X_{R_P}^{max})^4 + k_{s_{R_{P2}}}^{reg}} \times \frac{F}{CP_F}$	mmol P m^{-3} h^{-1}	R_P synthesis promoted by X_{S_P} and restricted by X_{R_P} (=R_P/(F/CP_F))
7	c_{R_P}	$k_{R_P}^{max} \times \frac{(1 - X_{S_P}/X_{S_P}^{max})^4}{(1 - X_{S_P}/X_{S_P}^{max})^4 + k_{c_{R_P}}^{reg}} \times R_P$	mmol P m^{-3} h^{-1}	R_P catabolism restricted by X_{S_P}
8	APA	$APA^{max} \times \frac{DOP}{DOP + k_{APA}} \times AP$	mmol P m^{-3} h^{-1}	Alkaline phosphatase activity as a function of DOP

Parameter values are shown in Table IV (for the new parameters in the model) and Supplementary data, Appendix C (for the parameters already used in AQUAPHY).

Table IV: Constant parameters related to P processes and APA for P. globosa

Parameters	Colony cells	Single cells	Units	Explanation	Reference
APA^{max}	3	3	mmol P mmol C^{-1} h^{-1}	Max. DOP hydrolysis rate at opt. T	Adjusted to satisfy Table I (v)
$h_{s_{AP}}$	8	8	–	Hill number of s_{AP} regulation by S_P	Adjusted to satisfy Table I (v, vi, vii)
k_{APA}	1.1	1.1	mmol P m^{-3}	Half-saturation constant of DOP hydrolysis	Xu *et al.* (2010)
$k_{c_{R_P}}^{reg}$	0.01	0.01	–	Half-saturation constant of c_{R_P} regulation by S_P	Based on Flynn *et al.* (1997)
$k_{deg_{AP}}$	0.25	0.25	h^{-1}	Spec. constant rate of AP degradation at opt. T	Based on Table I (ix)
k_P	0.3	0.3	mmol P m^{-3}	Half-saturation constant of P uptake	Based on Veldhuis *et al.* (1991) taking into account Table I (iv)
$k_{R_P}^{max}$	0.09	0.09	h^{-1}	Spec. constant rate of R_P catabolism at opt. T	Based on John and Flynn (2000)
$k_{s_{AP}}^{reg}$	0.001	0.001	–	Half-saturation constant of s_{AP} regulation by S_P	Adjusted to satisfy Table I (vi, vii, ix)
k_{S_P}	0.02	0.02	–	Half-saturation constant of P assimilation	Adjusted
$k_{s_{R_{P1}}}^{reg}$	0.01	0.01	–	Half-saturation constant of s_{R_P} regulation by S_P	Based on Flynn *et al.* (1997)
$k_{s_{R_{P2}}}^{reg}$	0.01	0.01	–	Half-saturation constant of s_{R_P} regulation by R_P	Based on Flynn *et al.* (1997)
$k_{upt_P}^{reg}$	0.01	0.01	–	Half-saturation constant of upt_{DIP} regulation by S_P	Based on Flynn *et al.* (1997)
s_{AP}^{max}	0.0009	0.0009	h^{-1}	Max. AP synthesis rate at opt. T	Adjusted to satisfy Table I (v)
$s_{R_P}^{max}$	0.18	0.18	h^{-1}	Max. R_P synthesis rate at opt. T	Based on John and Flynn (2000)
upt_P^{max}	0.44	0.22	h^{-1}	Max. transport rate of DIP at opt. T	Based on Veldhuis *et al.* (1991) taking into account Table I (iv)
$X_{S_P}^{max}$	0.2	0.2	–	Max. ratio between Sp and P included in F	Based on John and Flynn (2000)
$X_{R_P}^{max}$	1	1	–	Max. ratio between R_P and P included in F	Adjusted to satisfy Table I (ii)

(the ratio between S_P and the P contained in F, i.e. X_{S_P} = S_P/(F/CP_F)) while the N limitation is formulated by a hyperbolic function depending on the external DIN.

AP synthesis [s_{AP} in Equation (2) of Table III] depends on the availability of carbon monomers and of DIN, and is regulated by the internal soluble phosphate S_P. *De facto*, the demand for P from DOP, expressed through the synthesis of AP, is driven by internal P-stress in a mode analogous to (de)repression of metabolic pathways regulating AP synthesis in real organisms. The feedback control uses a sigmoidal function as described by Flynn *et al.* (Flynn *et al.*, 1997). Accordingly, AP synthesis is fully repressed when X_{S_P} reaches its maximum value $X_{S_P}^{max}$ and, in contrast, maximized when S_P is empty. Parameters (Hill number and half-saturation constant) have been adjusted in order to satisfy the available qualitative observations of AP regulation (Table I (vi, vii, viii)) and have been subjected to sensitivity analysis. First-order kinetics describes AP degradation [Equation (3) in Table III].

APA [Equation (8) in Table III] is controlled by the availability of DOP via Michaelis–Menten kinetics (Chróst and Overbeck, 1987). Hydrolysis of DOP via APA releases orthophosphate that contributes to the external DIP pool which is thence available for *P. globosa* (PO_{4APA}; Fig. 1A). Therefore, the success of APA in raising the internal P-status of the cells controls indirectly the synthesis of AP.

Energetic costs, as respiration [Equation (4) in Table III], include costs for cellular maintenance and synthesis of new functional and structural metabolites (including AP). The costs for F and AP synthesis are respectively proportional to μ and s_{AP} according to a metabolic cost function ξ varying as a function of the N source used, NO_3 or NH_4 [Equation (B8) in Supplementary data, Appendix B].

The internal pool of soluble inorganic phosphorus (S_P) is either directly supplied by DIP taken up from the ambient or indirectly by R_P catabolism. DIP uptake [Equation (5) in Table III] is a function of the external DIP and the internal S_P status considering that DIP uptake rate is maximum when X_{S_P} is zero and is down-regulated as X_{S_P} approaches its maximum size to prevent the pool from exceeding its maximum capacity. This is consistent with qualitative observations of DIP transport (Table I (i)). S_P also controls the R_P catabolism [Equation (7) in Table III] that is maximized when S_P is empty as a result of external DIP depletion, as suggested by existing observations relevant to P cell accumulation and consumption (Table I (iii)). The shape of these two regulating functions by S_P follows the arguments developed in Flynn *et al.* (Flynn *et al.*, 1997) and John and Flynn (John and Flynn, 2000), i.e. sigmoidal curves with a Hill number of 4 allow the simulation of pool regulation processes with realistic lag at high and low pool sizes. In contrast to DIP uptake, DIN uptake is controlled to support growth with fixed C:N stoichiometry for F, in agreement with Geider and Laroche (Geider and Laroche, 2002).

Loss processes include S_C excretion [Equation (B19) in Supplementary data, Appendix B] and cellular lysis, the latter being controlled by the nutrient stress [Equations (B16) and (B17) in Supplementary data, Appendix B]. Lysis of F supplies the external pool of DOP [Equation (B18) in Supplementary data, Appendix B] and the external pool of dead particulate organic P (dPOP) in equal proportions. In this model, the latter is a true sink that is not explicitly taken further into consideration. As bacterial hydrolysis of dPOP is not described in the model, dPOP is accumulated in the system. The process of colony disruption [Equations (B28) and (B29) in Supplementary data, Appendix B) releases single *P. globosa* cells whose dynamics is described by the same set of state variables and processes as colonial cells but without M (Supplementary data, Appendix A). Single cells are also able to synthesize AP under DIP limitation (Table I (v)) as observed by Veldhuis and Admiraal (Veldhuis and Admiraal, 1987). Total *P. globosa* biomass is calculated as the sum of colony and single cells biomass.

Parameters related to C and N metabolism (Supplementary data, Appendix C) are those of *P. globosa* in the MIRO model (Lancelot *et al.*, 2005) describing the planktonic ecosystem of the Southern North Sea and where phytoplankton dynamics are described by AQUAPHY. The new parameters describing the P metabolism (Table IV) have been determined on the basis of literature data and adjusted to satisfy the qualitative observations shown in Table I. The most important parameters on which experimental effort should be focused, were identified based on model sensitivity tests, making use of the method of Haefner (Haefner, 1996). The model was run under DIP-limiting (external DIP and DIN of, respectively, 1 mmol P m^{-3} and 110 mmol N m^{-3}) and DOP-enriched (1.5 mmol P m^{-3}) chemostat-type conditions. A normalized sensitivity index [SI, Equation (9)] based on steady-state biomass was then calculated for each parameter:

$$\mathrm{SI} = \frac{(\Upsilon - \Upsilon_{\mathrm{ref}})/\Upsilon_{\mathrm{ref}}}{(p - p_{\mathrm{ref}})/p_{\mathrm{ref}}} \qquad (9)$$

where Υ_{ref} is the value of *P. globosa* biomass reached at steady state with the reference parameter value p_{ref} (Table IV) and Υ is the value of *P. globosa* biomass reached at steady state with P, the reference parameter increased/decreased by 25 or 50%. The SI value is thus a measure of the relative variation of *P. globosa* biomass compared with the relative variation of the parameter (Haefner, 1996).

The simplified model (M2)

The structure of the simplified model (M2) is shown in Fig. 1B. By comparison to M1, it lacks an explicit description of the AP, the polyphosphate reserves R_P (at the level of cellular P-stress leading to the expression of AP, any polyphosphate would have already been exhausted), and the phosphate released from DOP hydrolysis (PO_{4APA}). However, APA is implicitly considered by allowing the direct uptake of DOP when DIP becomes limiting, i.e. upt_{DIP} calculated by Equation (5) in Table III becomes upt_P as follows:

$$\mathrm{upt_P} = \mathrm{upt_P^{max}} \times \frac{(\mathrm{DIP} + \mathrm{DOP})}{(\mathrm{DIP} + \mathrm{DOP}) + k_P} \times \frac{(1 - X_{S_P}/X_{S_P}^{\max})^4}{(1 - X_{S_P}/X_{S_P}^{\max})^4 + k_{\mathrm{upt_P}}^{\mathrm{reg}}} \times \frac{\mathrm{F}}{\mathrm{CP_F}} \qquad (10)$$

The proportions of DIP and DOP that are taken up are functions of (i) their respective concentrations and (ii) a preference function for DIP over DOP. Two different functions are tested to express that preference: f_{PCu} [Equation (11)] and f_{DIP} [Equation (13)] which distinguish two M2 versions: M2-f_{PCu} and M2-f_{DIP}. The first (f_{PCu}) is related to the C-biomass-based P-quota (PC), so that DOP use is zero when cells are P-replete ($PC = PC_{max}$) and increases as soon as PC declines towards PC_{min}. This function presents the advantage of being directly usable in the quota-based model (Flynn, 2008b) as well as in other models allowing a variable stoichiometry for phytoplankton such as the AQUAPHY model. Instead of calculating the preference function directly on the basis of PC (mmol P mmol C^{-1}), we calculate it on the basis of the dimensionless index of P-quota (PCu), ranging from 0 for starved to 1 for replete cells (Flynn, 2008a).

$$f_{PCu} = \frac{(1 - PCu)}{(1 - PCu) + k_{f_{PCu}}} \quad (11)$$

The dimensionless parameter $k_{f_{PCu}}$ [Equation (11)] has been estimated at 0.06 by fitting a hyperbolic function into the curve relating the C-biomass-specific AP normalized to the maximum specific AP and PCu, obtained with the mechanistic model M1 run in chemostat-type conditions at different dilution rates (Fig. 2). The dimensionless PCu is calculated as a function of PC by means of the normalized quota equation, as follows (Flynn, 2008a, b).

$$PCu = \frac{(1 + KQ)(PC - PC_{min})}{(PC - PC_{min}) + KQ(PC_{max} - PC_{min})} \quad (12)$$

In this model, PC is calculated as the ratio between P included in the F and S_P pools and C included in the F, S_C and R_C pools [i.e. $PC = (F/CP_F + S_P)/(F + S_C + R_C)$]. KQ is a dimensionless parameter controlling the shape of the "PCu vs. PC" curve, within minimum and maximum quota values (PC_{min}, PC_{max}). KQ reflects the manner in which an organism accumulates, distributes and uses the nutrient (Flynn, 2008b). For P limitation, KQ tends to be low (Flynn, 2008a), giving a strongly curved relationship, i.e. a significant decrease in PC from PC_{max} causes little stress initially. For this application, KQ was set at 0.3 (Flynn, 2008a).

The second function tested to express the preference for DIP over DOP [f_{DIP}; Equation (13)] is based on the external DIP, so that DOP uptake tends to zero when the external DIP is high.

$$f_{DIP} = 1 - \frac{DIP}{DIP + k_{f_{DIP}}} \quad (13)$$

The half-saturation constant for DOP uptake inhibition by DIP [$k_{f_{DIP}}$; Equation (13)] has been estimated at 0.2 mmol P m^{-3} by adjustment to fit with M1 results. This function has less physiological meaning than f_{PCu} as it is known that AP synthesis is directly controlled by the internal P status and not by the external DIP concentration (Myklestad and Sakshaug, 1983; Gage and Gorham, 1985; Lomas *et al.*, 2004; Dyhrman and Ruttenberg, 2006; Xu *et al.*, 2006; Litchman and Nguyen, 2008). However, this very simplified formulation could be applied to ecological models in which nutrient uptake relies only upon the external P, assuming a fixed stoichiometry for phytoplankton cells.

Sensitivity analysis of this simplified model has been performed with the same method as for M1.

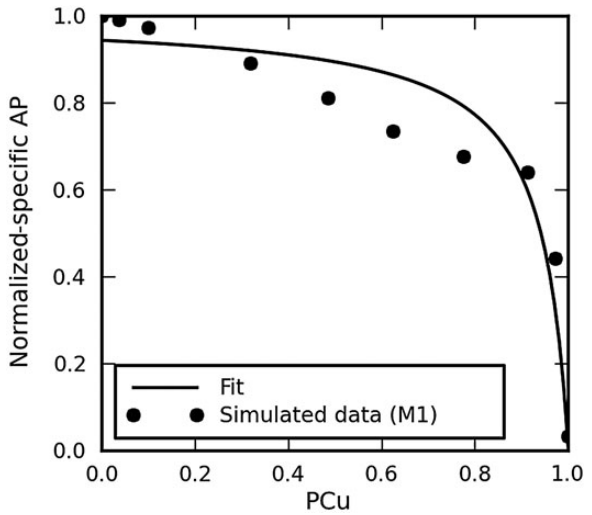

Fig. 2. Relationship between the C-biomass-specific AP normalized to the maximum specific AP and PCu, the index of P-status calculated as in Equation (12). This relationship was obtained using the mechanistic model M1 run to steady state at different dilution rates. The sigmoidal curve fitted by means of Microcal Origin 3.5 was used to parameterize the preference function for DIP over DOP [f_{PCu}; Equation (11)] as used in M2.

Model runs

In order to assess if the mechanistic model conforms to the qualitative observations (Table I), the model was run to simulate the evolution of the state variables in a 1-m-depth P-limited mesocosm under batch-type conditions over a period of 30 days with a time-step of 15 min. A sinusoidal 12/12 h light/dark cycle with a maximum incident light of 100 μmol quanta m^{-2} s^{-1} was imposed at the surface but varied in depth, depending on Chl *a*-dependent light attenuation coefficient [Equation (B3) in Supplementary data, Appendix B] and assuming a fixed C:Chl *a*

stoichiometry for F (Supplementary data, Appendix C). Temperature was kept constant at 10°C. The initial nutrient concentrations were selected to maintain a DIP nutrient limitation during the entire simulation (external DIP and DIN of, respectively. 1 mmol P m^{-3} and 110 mmol N m^{-3}). The initial DOP was zero but it was supplied by cell lysis during the experiment. The simulated mesocosm was seeded at time zero with colonies only (the first single cells being derived from colony disruption) with a biomass of 2.5 mmol C m^{-3}. The initial proportion of mucus M compared with cellular carbon ($F + AP + S_C + R_C$) was chosen to represent young forming colonies at bloom onset (Rousseau *et al.*, 1990). The AP, S_P and R_P pools were initially empty. These running conditions are hereafter referred to as reference conditions.

RESULTS

The mechanistic model (M1)

Model performance and sensitivity analysis

The performance of M1 was initially assessed by its ability to conform to the qualitative observations (Table I) in terms of AP synthesis and repression. Figure 3 shows the time evolution of *P. globosa* C-cell biomass (calculated as the sum of colony and single cells biomass), the distribution of P between DIP ($PO_4 + PO_{4APA}$), DOP, P-biomass and dPOP (calculated as the difference between the constant P-system and the other P pools), the C-biomass-based P-quota (PC) and the C-biomass-specific AP and APA simulated for the reference conditions. During the first 5 simulated days, *P. globosa* growth is sustained by inorganic nutrients initially present in the batch, leading to an increase of *P. globosa* biomass (Fig. 3A) also reflected in the P-biomass increase concomitant with a DIP decrease (Fig. 3B). During the same period, the DOP and dPOP concentration increase due to cell lysis (Fig. 3B). As S_P and R_P are initially empty, PC increases rapidly before being stable during the 5 first days (Fig. 3C). The AP synthesis being directly controlled by the S_P availability, the specific AP concentration initially increases but is then rapidly repressed when S_P is supplied by the external DIP (Fig. 3D). Despite this initial AP up-regulation, no APA is expressed because of the lack of its substrate, DOP (Fig. 3D). From Day 6, AP synthesis is up-regulated and

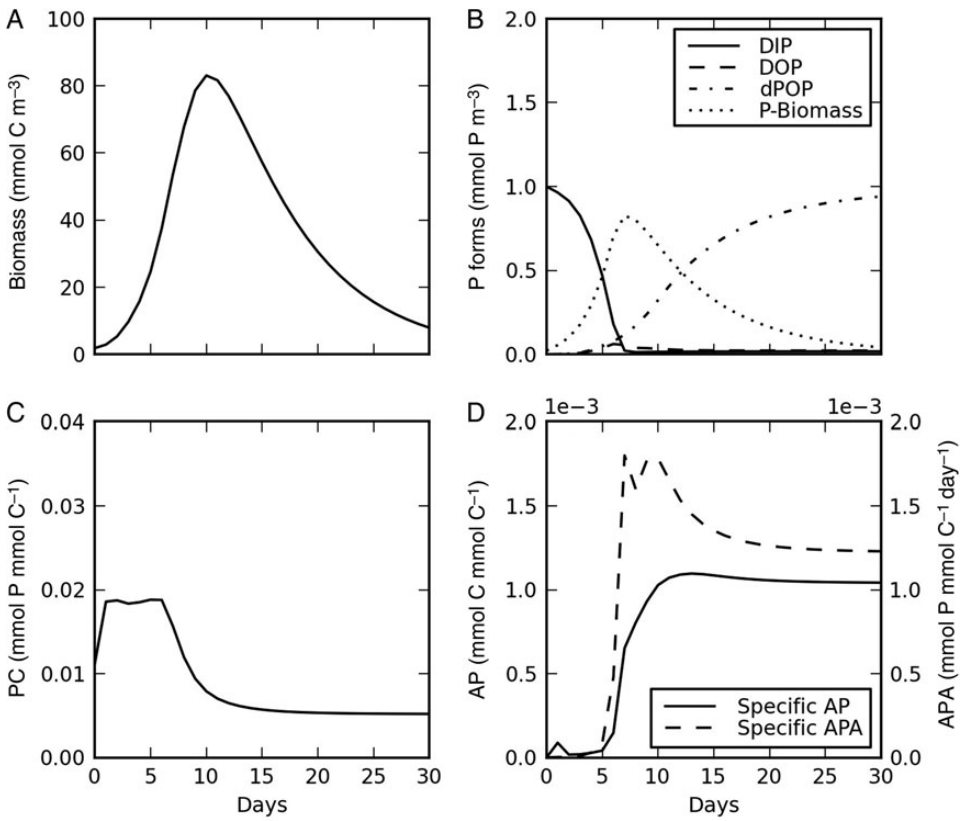

Fig. 3. Simulation under reference conditions. Time evolution (daily average values) of (**A**) *P. globosa* biomass (single + colony cells), (**B**) distribution of P between DIP ($PO_4 + PO_{4APA}$), DOP, dPOP (not described as a state variable in the model but calculated as the difference between the constant system-P and the other P pools) and biomass-P, (**C**) C-biomass-based P-quota (PC) excluding the mucus and (**D**) C-biomass-specific AP and C-biomass-specific APA.

C-biomass-specific AP concentration starts to increase (Fig. 3D). This occurs in the late exponential phase of *P. globosa* growth (Fig. 3A) in agreement with observations of APA occurrence in *E. huxleyi* (Table I (vi)) and when PC starts to decrease because of the DIP stress (Fig. 3C). The value of DIP at which AP synthesis is up-regulated in the simulation (i.e. 0.2 mmol P m^{-3}; Fig. 3B) is similar to that observed by Veldhuis *et al.* (Veldhuis *et al.*, 1987) in natural populations of *P. globosa*. This threshold value is constant whatever the initial DIP concentration (not shown). DOP decreases through expressed APA (Fig. 3C and D). Because of the low DOP concentration, the PO_{4APA} released by APA supports simulated *P. globosa* growth during 4 additional days. From Day 10, R_P has been entirely catabolized and the ambient DOP is too low to support growth. Thereafter, loss terms become higher than growth terms and the biomass starts to decrease (Fig. 3A). At that time, PC is mainly controlled by F, S_C and R_C and the ratio becomes stable at 0.005 mmol P mmol C^{-1} (Fig. 3C). The constant lack of S_P maintains the specific AP at a high value (Fig. 3D). The apparent DIP and DOP equilibrium at 0.022 mmol P m^{-3} (Fig. 3B) results from the balance between the PO_{4APA} supply by APA and its consumption by *P. globosa*, and between the DOP supply by cell lysis and its hydrolysis by the AP synthesized by still living P-limited cells.

The ability of the model to describe the expected repression of AP synthesis when DIP is re-supplied in DIP-limited culture (Table I (ix)) is tested by adding 2.5 mmol P-DIP m^{-3} on Day 10, i.e. when DIP is depleted (Fig. 4). Results show that PC increases immediately upon DIP addition (Fig. 4C) showing that the filling of S_P and R_P is rapid and therefore specific AP concentration also decreases immediately upon DIP addition leading to a decrease of APA (Fig. 4B and D). The added DIP allows *P. globosa* to increase threefold its maximum biomass. AP synthesis is then de-repressed when DIP is depleted again satisfying the observation that APA responds rapidly to fluctuations in DIP level provided DOP is available (Table I (vii)). The decline of *P. globosa* biomass coincides here with DIN depletion (not shown) that also controls AP synthesis and thus explains the zero

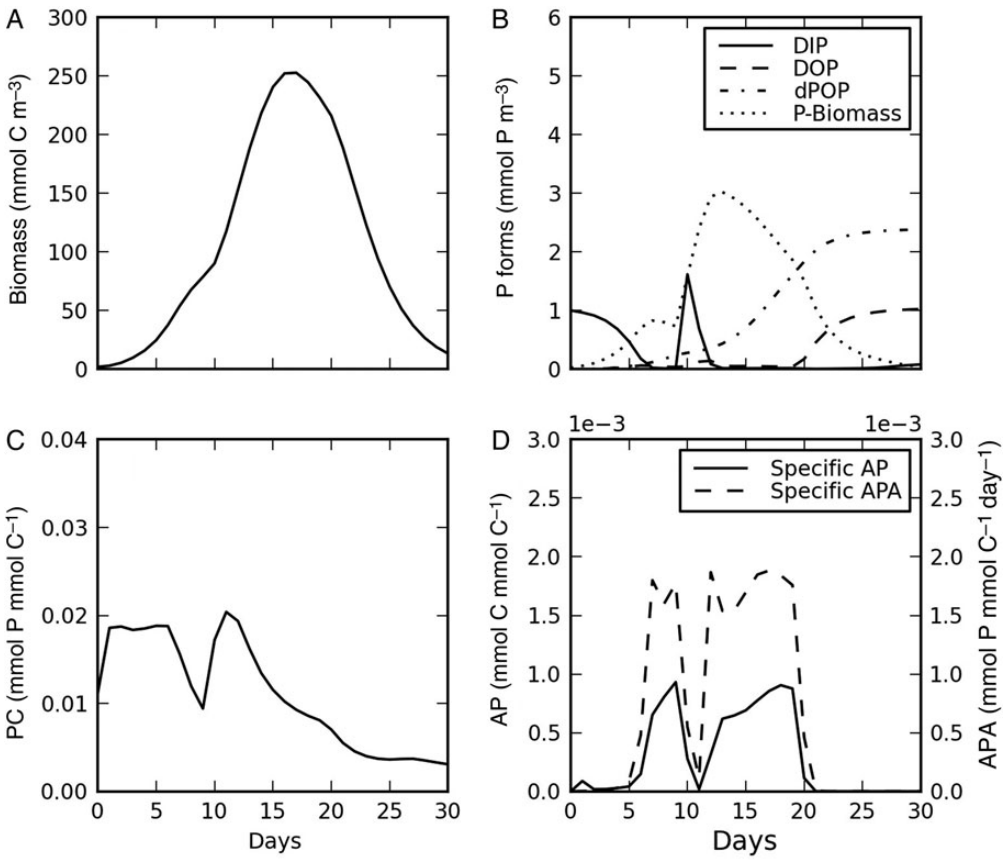

Fig. 4. Simulation under reference conditions with a pulse of 2.5 mmol P-DIP m^{-3} on Day 10. Time evolution (daily average values) of (**A**) *P. globosa* biomass (single + colony cells), (**B**) Distribution of P between DIP (PO_4 + PO_{4APA}), DOP, dPOP (not described as a state variable in the model but calculated as the difference between the constant system-P and the other P pools) and biomass-P, (**C**) C-biomass-based P-quota (PC) excluding the mucus and (**D**) C-biomass-specific AP and C-biomass-specific APA.

value of the C-biomass-specific AP (and APA) from Day 21 (Fig. 4D). This DIN limitation also explains the increase of DOP and, to a lesser extent, DIP from Day 19 and 21, respectively, due to cellular lysis releasing DOP from F lysis and DIP from S_P and R_P lysis (Fig. 4B).

Altogether these results show that behaviour of the mechanistic model accords with existing qualitative observations related to P metabolism and APA of *P. globosa* specifically, or of haptophytes in general (as summarized in Table I).

Introduction of an explicit description of AP in the AQUAPHY model introduces new parameters. Of these, only 6 are directly related to AP up-regulation and activity while 11 others are related to the S_P and R_P intracellular pools needed for describing the regulation of AP synthesis by the internal orthophosphate (S_P). As most of these new parameters are not accurately known for *P. globosa*, a sensitivity analysis was conducted to determine the key parameters on which special attention should be placed. Accordingly, each parameter was increased and decreased by 50 and 25%, and the resulting average SI was calculated making use of Equation (9). As the same conclusions could be drawn with results obtained after a 25 and a 50% change (except that SI values were lower with a 25% change), only the SI obtained with a 50% change are presented (Fig. 5A).

The five most sensitive parameters (i.e., (k_{S_P}, $X^{max}_{S_P}$, $X^{max}_{R_P}$, $s^{max}_{R_P}$ and $k^{max}_{S_P}$) show an SI between 0.08 and 0.33, meaning that a 50% change of the reference parameter induces only a $\pm 4-16.5\%$ change of the *P. globosa* biomass reached at steady state. The computed SI of the 12 remaining range from 0.0006 to 0.06, meaning that a 50% change of their reference value induces only a 0.03 to $\pm 3\%$ change of the *P. globosa* biomass reached at steady state. The operation of the model is thus largely insensitive to the selection of parameter values, providing a robust structure. It is interesting to note that the five parameters that influence the steady-state biomass the most are not involved in the description of AP synthesis and activity. $X^{max}_{S_P}$ and k_{S_P} control directly the P available for synthesis of new metabolites; the former determining the maximum S_P concentration and the latter determining the ability to assimilate S_P in new metabolites. It is thus expected that they have an important effect on *P. globosa* biomass under P limiting conditions and special emphasis should be given to determining these parameters experimentally. Similarly, $X^{max}_{R_p}$, $s^{max}_{R_p}$ and k_{R_p} are key parameters as they

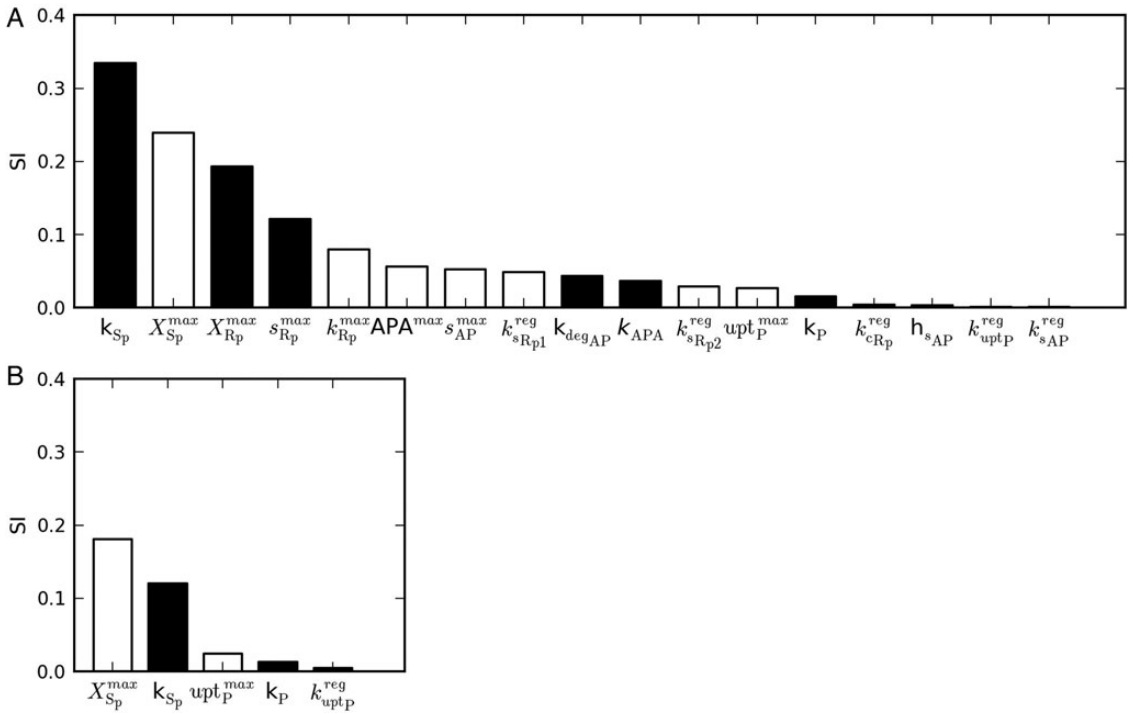

Fig. 5. Ranking of model parameters based on their normalized sensitivity index (SI) calculated as in Equation (9) for a 50% change of the parameter value. White bars are parameters for which the model response (*P. globosa* biomass) is positive when the parameter value is increased. Black bars are parameters for which the model response is negative when the parameter value is increased. SI = 1 indicates a pro-rata relationship between change in parameter value and impact on biomass. (**A**) SI obtained with the mechanistic model M1, (**B**) SI obtained with the simplified model M2. See Table IV for full description of parameters.

control indirectly the DIP available for the synthesis of new metabolites by affecting the competition for P use between the latter process and the accumulation of polyphosphates.

Significance of APA

The significance of APA for *P. globosa* growth was explored by comparing model simulations in which the potential to synthesize AP is turned on and off. Simulations were performed under reference conditions except for initial DOP varying between 0 and 1.5 mmol P m^{-3}, the maximal value observed in the Southern North Sea during spring (unpublished data). The resulting evolution of *P. globosa* biomass, DIP, DOP and PC is shown in Fig. 6. When the ability to synthesize AP is turned off, the *P. globosa* biomass starts to decrease from Day 9 (Fig. 6A) when ambient DIP is depleted (Fig. 6B) and R_P has been entirely catabolized to support growth (Fig. 6C). Simultaneously DOP accumulates, supplied by cell lysis (Fig. 6D). When AP synthesis is turned on, the PO_{4APA} released from DOP supports net growth during a longer period and allows a higher maximum biomass (Fig. 6A). The cost related to AP synthesis does not significantly impact the maximum biomass attained as it never exceeds 4% of the cost related to μ during the net growth period. For the three simulations, APA is triggered on Day 6 regardless of the initial DOP concentration (observed from the simulated DOP decrease in Fig. 6D). In contrast, the initial DOP level determines the maximum *P. globosa* biomass attainable, being 1.3–3 times higher when the model has the potential to express AP than without this potential (Fig. 6A). The initial DOP level also determines the duration of the net growth period that tends to be longer when initial DOP is higher (Fig. 6A). Regarding cellular stoichiometry, it can be observed that when initial DOP is sufficient, AP up-regulation allows the maintenance of an elevated PC over a longer period (Fig. 6C) because the external DIP provided by DOP hydrolysis is sufficient to support growth without using internal P reserves during 2–3

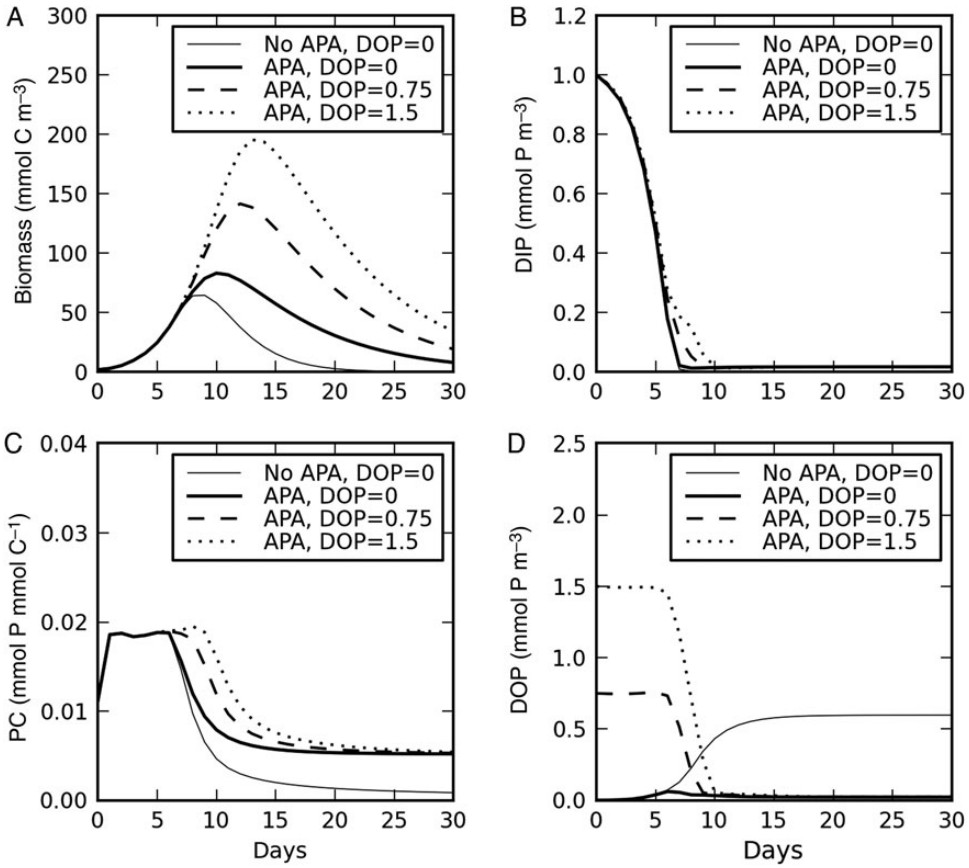

Fig. 6. Simulations under reference conditions with and without APA ability and with different initial DOP concentrations (0, 0.75 and 1.5 mmol P m^{-3}). Time evolution (daily average values) of (**A**) *P. globosa* biomass (single + colony cells), (**B**) DIP (PO_4 + PO_{4APA}), (**C**) C-biomass-based P-quota (PC) and (**D**) DOP. DOP is recycled in the system through cell lysis [Equation (B18) in Supplementary data, Appendix B]; hence, the DOP accumulation when APA ability is turned off.

days. Additionally, at the end of the simulation, the PC value is stable at 0.005 mmol P mmol C^{-1} for the three simulations allowing AP up-regulation, whereas the PC value is lower by a factor 5 in the absence of AP up-regulation (Fig. 6C).

Significance of the P reserve pool

The capacity of *P. globosa* to accumulate polyphosphates has been reported as modest (Jahnke, 1989; Table I (ii)) justifying the small $X_{R_P}^{max}$ value used here (Table IV). However, there are reports of large variability in the capacity to accumulate polyphosphates ($X_{R_P}^{max}$) among phytoplankton species/classes (Harold, 1966; Riegman *et al.*, 2000; Sterner and Elser, 2002), a feature of importance in competition (John and Flynn, 2000; Flynn, 2002).

In order to test the competitive advantage of holding a high capacity to accumulate polyphosphate coupled with an ability to express APA, simulations were performed under reference conditions with three configurations describing hypothetical phytoplankton species differing in respect of their $X_{R_P}^{max}$ value and competing for the same P resource. The $X_{R_P}^{max}$ values were chosen to cover the plausible range of R_P capacity based on the observation that the P reserve can be responsible for a 2.5 times higher PC than in the absence of P reserve (John and Flynn, 2000). Results (Fig. 7) show that $X_{R_P}^{max}$ impacts directly the PC, with a maximum PC being 1.6 times higher when $X_{R_P}^{max}$ is increased from 0.1 to 2.5 (Fig. 7C). When external DIP and DOP are too low to sustain growth (on Day 8; Fig. 7B and D) a configuration with higher $X_{R_P}^{max}$ value are able to maintain growth during a longer period and can reach a higher maximum biomass (Fig. 7A) thanks to R_P catabolism (Fig. 7C).

The simplified model (M2)

The performance of the simplified model M2 was assessed by comparing its results in terms of biomass and nutrient dynamics with those obtained by the mechanistic model M1 conforming to the qualitative knowledge of P metabolism and AP up-regulation. M1 and M2 were all run to simulate the evolution of state variables in

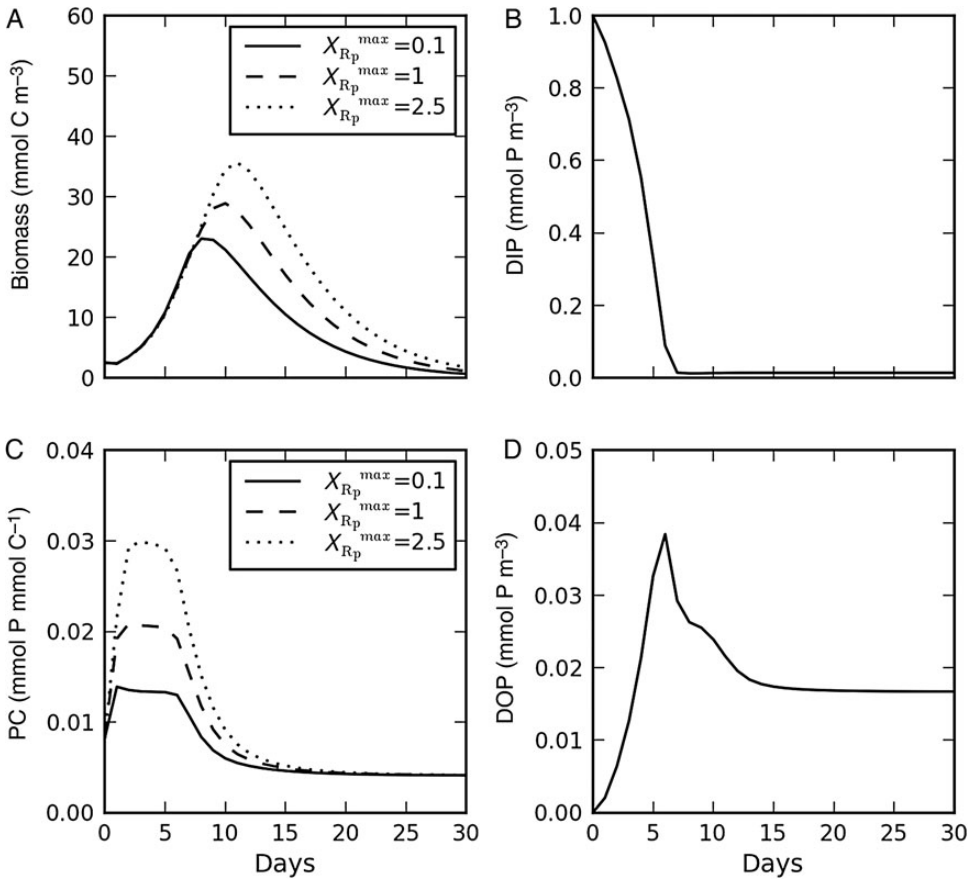

Fig. 7. Simulation under reference conditions with three configurations describing hypothetical phytoplankton species differing by their ability to accumulate polyphosphates ($X_{R_P}^{max}$ = 0.1, 1, 2.5) and competing for the same nutrient resources. Time evolution (daily average values) of (**A**) phytoplankton biomass, (**B**) DIP (PO_4 + PO_{4APA}), (**C**) C-biomass-based P-quota (PC) and (**D**) DOP.

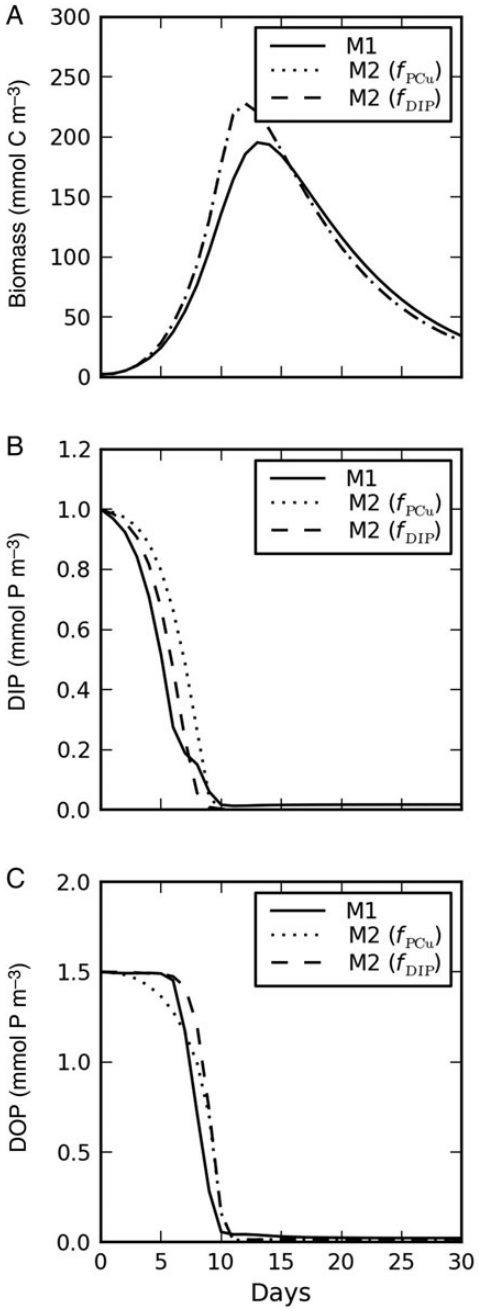

Fig. 8. Comparison between outputs from the three alternative models simulating the time evolution (daily average values) of (**A**) *P. globosa* biomass, (**B**) ambient DIP and (**C**) DOP, in DIP-limiting and DOP-enriched conditions. M1: mechanistic model (Fig. 1A); M2 − f_{PCu}: simplified model without R_P and AP (Fig. 1B) with proportions of DOP and DIP taken up controlled by the PCu. M2 − *f*DIP: simplified model without R_P and AP (Fig. 1B) with proportions of DOP and DIP taken up controlled by the external DIP.

DIP-limited (external DIP and DIN of, respectively, 1 mmol P m^{-3} and 110 mmol N m^{-3}) and DOP-enriched (1.5 mmol P m^{-3}) batch-type conditions. In order to quantify the similarity between simulations obtained with M1 and M2, three statistics were computed as in Taylor (Taylor, 2001): the correlation coefficient (r) quantifying pattern similarity, the centred pattern root mean square (E') quantifying differences, and the variances ratio of the two simulations (σ_{M2}/σ_{M1}). Figure 8 compares the time evolution of *P. globosa* biomass, DIP and DOP simulated with M1, M2-f_{PCu} and M2-f_{DIP}. The evolution of *P. globosa* biomass is exactly the same for M2-f_{PCu} and M2-f_{DIP} (Fig. 8A) because the total P uptake rate is calculated in the same way for the two formulations (the only difference between the two formulations is the calculation of the proportion of DIP vs. DOP that are taken up). Statistically, the evolution of *P. globosa* biomass simulated by M2 is very close to that obtained with M1 ($r = 0.98$, $E' = 0.26$, $\sigma_{M2}/\sigma_{M1} = 1.13$). The slightly faster growth rate simulated with M2 as well as the slower DIP and DOP consumption (Fig. 8B and C) are explained by the absence of the explicit description of R_P. In terms of DIP consumption, the two M2 formulations reproduce correctly the result obtained with M1 (Fig. 8B) even if M2-f_{DIP} appeared to be slightly more efficient, based on the three statistics [$r = 0.99$ (vs. 0.96 with M2-f_{PCu}), $E' = 0.17$ (vs. 0.32 with M2-f_{PCu}), $\sigma_{M2}/\sigma_{M1} = 1.09$ (vs. 1.16 with M2-f_{PCu})]. In contrast, the three statistics show that M2-f_{PCu} is slightly more efficient than M2-f_{DIP} to simulate the DOP consumption [$r = 0.99$ (vs. 0.98 with M2-f_{DIP}), $E' = 0.16$ (vs. 0.2 with M2-f_{DIP}), $\sigma_{M2}/\sigma_{M1} = 0.98$ (vs. 1.05 with M2-f_{DIP})].

Taken together, we can conclude that a simplified formulation of APA ability gives very satisfactory results in terms of biomass and nutrient dynamics. Furthermore, the sensitivity analysis performed with the same method as for M1 shows that the simplified model is more robust in parameter changes than M1 (Fig. 5B).

DISCUSSION

Phosphatase (with acid or alkaline optima) is a very common extracellular enzyme expressed by microbes growing in aquatic environments. Its existence is indicative of the importance of P-availability for biological activity and the relative abundance of DOP as the substrate. It is thus surprising that hitherto there has been no attempt to include expression of phosphatase in models of plankton. The present work shows the first mechanistic model explicitly describing the (de)repressive regulation of AP in agreement with qualitative observations related to DIP transport, intracellular accumulation of polyphosphate and AP induction and activity. By the choice of the physiological parameters and the description of the mucus surrounding colonies, the model specifically describes the haptophyte *P. globosa* known to be able to

synthesize AP (Veldhuis and Admiraal, 1987; van Boekel and Veldhuis, 1990; Veldhuis *et al.*, 1991) and suspected to use DOP to sustain its growth when DIP is very low (Rousseau *et al.*, 2004; Lancelot *et al.*, 2005). Unfortunately, there are no suitable published batch experimental data available to enable a full assessment of our mechanistic model. This is because, as previously noted (Flynn, 2005), experiments typically do not collect data of the type, or with the appropriate units, suitable for modelling. For example, the initial state of the P reserves, total cellular C:N:P, and the precise initial number of cells are typically not recorded (e.g. Veldhuis and Admiraal, 1987; van Boekel and Veldhuis, 1990; Veldhuis *et al.*, 1991; Dyhrman and Palenik, 2003; Xu *et al.*, 2006).

When the mechanistic model is used to simulate DIP-limiting and DIN-enriched conditions, as typically observed today in some coastal ecosystems, it shows that the explicit consideration of APA ability can significantly increase phytoplankton biomass building if DOP is available (Fig. 6). This is supported by many field studies suggesting that DOP can be of major importance to sustain productivity in DIP-limited coastal (e.g. Nausch, 1998; Labry *et al.*, 2005; Nicholson *et al.*, 2006; Bogé *et al.*, 2012) and also oceanic (Vidal *et al.*, 2003; Sohm and Capone, 2006; Mather *et al.*, 2008; Duhamel *et al.*, 2010; Lomas *et al.*, 2010) ecosystems. More specifically, Lomas *et al.* (Lomas *et al.*, 2010) suggest that DOP hydrolysis would provide ~60% of the estimated annual P demand in the Sargasso Sea and Mather *et al.* (Mather *et al.*, 2008) found that 30% of the primary production was supported by DOP in the North Atlantic gyre during the boreal spring. In addition to field evidence, some modelling studies also highlight the importance of including an explicit DOP pool in ecological models (Salihoglu *et al.*, 2007) as well as an explicit ability of DOP uptake by the phytoplankton (Letscher and Moore, 2015).

To properly explore competitive advantages between phytoplankton using DOP, it is necessary to consider the mechanisms used for exploitation of the resource. Indeed, species up-regulate expression at different rates (Kuenzler and Perras, 1965) and different levels of expression, not only to DOP in general (APA) but also to more specific fractions of DOP (Flynn *et al.*, 1986). The AP production rate has been shown to be particularly high for haptophytes (Kuenzler and Perras, 1965). As phosphatases are cell-bound enzymes, it is reasonable to assume that the DIP released from DOP hydrolysis is immediately transferred into the cell and is thus not so readily available for other (competing) organisms. Therefore, the ability to synthesize AP at a high rate may give a substantial competitive advantage over other species in DIP-limiting environments. This competitive advantage may be reinforced or counterbalanced by the nutrient transport efficiency and/or by the ability to accumulate internal P reserves under the form of polyphosphates (Flynn, 2002). Several studies show that some species can exhibit surge DIP transport capacities under DIP-limiting conditions, leading to rapid filling of the internal P reserves and rapid DIP depletion (Falkner *et al.*, 1998; Riegman *et al.*, 2000; Wagner *et al.*, 2000). In this respect *P. globosa*, with a maximum DIP uptake rate lower by 1−2 orders of magnitude compared with other species (see Riegman *et al.*, 2000), is not particularly competitive and this explains the ~12 h needed to fill the internal P reserve (Figs 3C, 4C, 6C and 7C). The competitive advantage of holding a large capacity to accumulate P reserves has been tested with the mechanistic model simulating competition between three hypothetical configurations differing only by their maximum P reserve capacity. It shows that species able to accumulate larger P reserves can grow for a longer period which could be a major advantage in short-term transient events of DIP supply as discussed in John and Flynn (John and Flynn, 2000).

The explicit representation of the ability of phytoplankton to use DOP as a P source is needed in ecological/biogeochemical models describing DIP-limiting ecosystems. However, such a detailed description of the AP up-regulation might not be necessary or desirable when considering the added computational load. Therefore, we present a simplified formulation (M2) derived from the mechanistic model (M1) but involving fewer state variables and parameters. However, it is worth noting that the mechanistic model, with feedback interactions, does not conform to stereotypic "complex models" with respect to the numbers of parameters. In reality, most parameters in these types of models control well-constrained processes; hence, the low sensitivities (SI <0.1; Fig. 5A) to the selection of P parameter values (Fasham *et al.*, 2006). We distinguished two versions of M2 (M2-f_{PCu} and M2-f_{DIP}) according to the function used to calculate the preference for DIP over DOP [f_{PCu}; Equation (11) or f_{DIP}; Equation (13)]. With M2-f_{PCu}, the proportions of DIP and DOP that are taken up depend on the internal P-status of the cells while it depends only on the external DIP concentration with M2-f_{DIP} The comparison between the simplified model (M2) and the mechanistic model (M1) has shown that the simplified model gives very satisfactory results in terms of biomass and nutrient dynamics (Fig. 8). However, the choice between the two formulations expressing the proportion of DIP and DOP consumed by phytoplankton cannot be made on the basis of these results but rather depends on the type of model used. As M2-f_{PCu} has a better physiological meaning, this formulation should be favoured in ecological models allowing a variable stoichiometry for phytoplankton cells as quota-based models and AQUAPHY-based models. For those models with a fixed

phytoplankton stoichiometry, M2-f_{DIP} could be applied, but only in systems where P is the sole limiting nutrient.

SUPPLEMENTARY DATA

Supplementary data can be found online at http://plankt.oxfordjournals.org.

FUNDING

C.G. benefits from a PhD scholarship funded by the Fonds de la Recherche Scientifique (F.R.S.- FNRS, Belgium). This work is a contribution to the EMOSEM (Ecosystem Models as Support to Eutrophication Management in the North Atlantic Ocean) EU FP7 Eranet Seas ERA project funded by the Belgian Science Policy (BELSPO). The contribution of K.J.F. was supported via a Leverhulme Trust International Network grant.

REFERENCES

Billen, G., Garnier, J. and Rousseau, V. (2005) Nutrient fluxes and water quality in the drainage network of the Scheldt basin over the last 50 years. *Hydrobiologia*, **540**, 47–67.

Bogé, G., Lespilette, M., Jamet, D. and Jamet, J. L. (2012) Role of sea water DIP and DOP in controlling bulk alkaline phosphatase activity in N.W. Mediterranean Sea (Toulon, France). *Mar. Pollut. Bull.*, **64**, 1989–1996.

Bonachela, J. A., Allison, S. D., Martiny, A. C. and Levin, S. A. (2013) A model for variable phytoplankton stoichiometry based on cell protein regulation. *Biogeosciences*, **10**, 4341–4356.

Cembella, A. D., Antia, N. J. and Harrison, P. J. (1984) The utilization of inorganic and organic phosphorous compounds as nutrients by eukaryotic microalgae: a multidisciplinary perspective: part 1. *Crit. Rev. Microbiol.*, **10**, 317–391.

Chróst, R. J. and Overbeck, J. (1987) Kinetics of alkaline phosphatase activity and phosphorus availability for phytoplankton and bacterioplankton in Lake Plußsee (North German Eutrophic Lake). *Microb. Ecol.*, **13**, 229–248.

Duhamel, S., Dyhrman, S. T. and Karl, D. M. (2010) Alkaline phosphatase activity and regulation in the North Pacific Subtropical Gyre. *Limnol. Oceanogr.*, **55**, 1414–1425.

Dyhrman, S. T., Jenkins, B. D., Rynearson, T. A., Saito, M. A., Mercier, M. L., Alexander, H., Whitney, L. P., Drzewianowski, A. *et al.* (2012) The transcriptome and proteome of the diatom *Thalassiosira pseudonana* reveal a diverse phosphorus stress response. *PLoS One*, **7**, e33768.

Dyhrman, S. T. and Palenik, B. (2003) Characterization of ectoenzyme activity and phosphate-regulated proteins in the coccolithophorid *Emiliania huxleyi*. *J. Plankton Res.*, **25**, 1215–1225.

Dyhrman, S. T. and Ruttenberg, K. C. (2006) Presence and regulation of alkaline phosphatase activity in eukaryotic phytoplankton from the coastal ocean: implications for dissolved organic phosphorus remineralization. *Limnol. Oceanogr.*, **51**, 1381–1390.

Falkner, R., Wagner, F., Aiba, H. and Falkner, G. (1998) Phosphate-uptake behaviour of a mutant of *Synechococcus* sp. PCC 7942 lacking one protein of the high-affinity phosphate-uptake system. *Planta*, **206**, 461–465.

Fasham, M. J. R., Flynn, K. J., Pondaven, P., Anderson, T. R. and Boyd, P. W. (2006) Development of a robust ecosystem model to predict the role of iron on biogeochemical cycles: a comparison of results for iron-replete and iron-limited areas, and the SOIREE iron-enrichment experiment. *Deep Sea Res Part I*, **53**, 333–366.

Flynn, K. J. (2002) How critical is the critical N:P ratio? *J. Phycol.*, **38**, 961–970.

Flynn, K. J. (2005) Castles built on sand; dysfunctional plankton models and the failure of the biology-modelling interface. *J. Plankton Res.*, **27**, 1205–1210.

Flynn, K. J. (2008a) The importance of the form of the quota curve and control of non-limiting nutrient transport in phytoplankton models. *J. Plankton Res.*, **30**, 423–438.

Flynn, K. J. (2008b) Use, abuse, misconceptions and insights from quota models: the Droop cell-quota model 40 years on. *Oceanogr. Mar. Biol. Ann. Rev.*, **46**, 1–23.

Flynn, K. J., Fasham, M. J. R. and Hipkin, C. R. (1997) Modelling the interactions between ammonium and nitrate uptake in marine phytoplankton. *Phil. Trans. R. Soc., B*, **352**, 1625–1645.

Flynn, K. J., Öpik, H. and Syrett, P. J. (1986) Localization of the alkaline phosphatase and 5′nucleotidase activities of the diatom *Phaeodactylum tricornutum*. *J. Gen. Microbiol.*, **132**, 289–298.

Gage, M. A. and Gorham, E. (1985) Alkaline phosphatase activity and cellular phosphorus as an index of the phosphorus status of phytoplankton in Minnesota Lakes. *Freshwater Biol.*, **15**, 227–233.

Geider, R. and Laroche, J. (2002) Redfield revisited: variability of C:N:P in marine microalgae and its biochemical basis. *Eur. J. Phycol.*, **37**, 1–17.

Glibert, P. M. and Legrand, C. (2006) The diverse nutrient strategies of harmful algae: focus on osmotrophy. In: Granéli, E. and Turner, J. T. (eds), *Ecology of Harmful Algae. Ecol. Stud.*, 189, Springer, Berlin, pp. 163–175.

Gobler, C. J., Berry, D. L., Dyhrman, S. T., Wilhelm, S. W., Salamov, A., Lobanov, A. V., Zhang, Y., Collier, J. L. *et al.* (2011) Niche of harmful alga *Aureococcus anophagefferens* revealed through ecogenomics. *Proc. Natl. Acad. Sci. USA*, **108**, 4352–4357.

Haefner, J. W. (1996) *Modelling Biological Systems: Principles and Applications*. Chapman & Hall, New York.

Harold, F. M. (1966) Inorganic polyphosphates in biology: structure, metabolism, and function. *Bacteriol. Rev.*, **30**, 772–794.

Hoppe, H. G. (2003) Phosphatase activity in the sea. *Hydrobiologia*, **493**, 187–200.

Jahnke, J. (1989) The light and temperature dependence of growth rate and elemental composition of *Phaeocystis globosa* Scherffel and *P. pouchetii* (Har.) Lagerh. in batch cultures. *Neth. J. Sea. Res.*, **23**, 15–21.

John, E. H. and Flynn, K. J. (2000) Modelling phosphate transport and assimilation in microalgae; how much complexity is warranted? *Ecol. Model.*, **125**, 145–157.

Klausmeier, C. A., Litchman, E. and Levin, S. A. (2007) A model of flexible uptake of two essential resources. *J. Theor. Biol.*, **246**, 278–289.

Kuenzler, E. J. and Perras, J. P. (1965) Phosphatases of marine algae. *Biol. Bull.*, **128**, 271–284.

Labry, C., Delmas, D. and Herbland, A. (2005) Phytoplankton and bacterial alkaline phosphatase activities in relation to phosphate and

DOP availability within the Gironde plume waters (Bay of Biscay). *J. Exp. Mar. Biol. Ecol.*, **318**, 213–225.

Lancelot, C., Billen, G., Sournia, A., Weisse, T., Colijn, F., Veldhuis, M. J. W., Davies, A. and Wassman, P. (1987) *Phaeocystis* blooms and nutrient enrichment in the continental coastal zones of the North Sea. *Ambio*, **16**, 38–46.

Lancelot, C. (1995) The mucilage phenomenon in the continental coastal waters of the North Sea. *Sci. Total Environ.*, **165**, 83–102.

Lancelot, C. and Mathot, S. (1985) Biochemical fractionation of primary production by phytoplankton in Belgian coastal waters during short- and long-term incubations with ^{14}C-bicarbonate. II. *Phaeocystis poucheti* colonial population. *Mar. Biol.*, **86**, 227–232.

Lancelot, C., Spitz, Y., Gypens, N., Ruddick, K., Becquevort, S., Rousseau, V., Lacroix, G. and Billen, G. (2005) Modelling diatom and *Phaeocystis* blooms and nutrient cycles in the Southern Bight of the North Sea: the MIRO model. *Mar. Ecol. Prog. Ser.*, **289**, 63–78.

Lancelot, C., Veth, C. and Mathot, S. (1991) Modelling ice-edge phytoplankton bloom in the Scotia-Weddell sea sector of the Southern Ocean during spring 1988. *J. Mar. Syst.*, **2**, 333–346.

Letscher, R. T. and Moore, J. K. (2015) Preferential remineralization of dissolved organic phosphorus and non-Redfield DOM dynamics in the global ocean: impacts on marine productivity, nitrogen fixation, and carbon export. *Glob. Biogeochem. Cycles*, doi:10.1002/2014GB004904.

Litchman, E. and Nguyen, B. L. V. (2008) Alkaline phosphatase activity as a function of internal phosphorus concentration in freshwater phytoplankton. *J. Phycol.*, **44**, 1379–1383.

Lomas, M. W., Bonachela, J. A., Levin, S. A. and Martiny, A. C. (2014) Impact of ocean phytoplankton diversity on phosphate uptake. *PNAS*, **111**, 17540–17545.

Lomas, M. W., Burke, A. L., Lomas, D. A., Bell, D. W., Shen, C., Dyhrman, S. T. and Ammerman, J. W. (2010) Sargasso Sea phosphorus biogeochemistry: an important role for dissolved organic phosphorus (DOP). *Biogeosciences*, **7**, 695–710.

Lomas, M. W., Swain, A., Shelton, R. and Ammerman, J. W. (2004) Taxonomic variability of phosphorus stress in Sargasso Sea phytoplankton. *Limnol. Oceanogr.*, **49**, 2303–2310.

Mather, R. L., Reynolds, S. E., Wolff, G. A., Williams, R. G., Torres-Valdes, S., Woodward, E. M. S., Landolfi, A., Pan, X. *et al.* (2008) Phosphorus cycling in the North and South Atlantic Ocean subtropical gyres. *Nat. Geosci.*, **1**, 439–443.

Mitra, A., Flynn, K. J., Burkholder, J. M., Berge, T., Calbet, A., Raven, J. A., Granéli, E., Hansen, P. J. *et al.* (2014) The role of mixotrophic protists in the biological carbon pump. *Biogeosciences*, **11**, 1–11.

Myklestad, S. and Sakshaug, E. (1983) Alkaline phosphatase activity of *Skeletonema costatum* populations in the Trondheimsfjord. *J. Plankton Res.*, **5**, 557–564.

Nausch, M. (1998) Alkaline phosphatase activities and the relationship to inorganic phosphate in the Pomeranian Bight (southern Baltic Sea). *Aquat. Microb. Ecol.*, **16**, 87–94.

Nicholson, D., Dyhrman, S., Chavez, F. and Paytan, A. (2006) Alkaline phosphatase activity in the phytoplankton communities of Monterey Bay and San Francisco Bay. *Limnol. Oceonogr.*, **51**, 874–883.

Pahlow, M. and Oschlies, A. (2009) Chain model of phytoplankton P, N and light colimitation. *Mar. Ecol. Prog. Ser.*, **376**, 69–83.

Passy, P., Gypens, N., Billen, G., Garnier, J., Thieu, J., Rousseau, V., Callens, J., Parent, J. Y. *et al.* (2013) A model reconstruction of riverine nutrient fluxes and eutrophication in the Belgian Coastal Zone (Southern North Sea) since 1984. *J. Mar. Syst.*, **128**, 106–122.

Riegman, R., Stolte, W., Noordeloos, A. A. M. and Slezak, D. (2000) Nutrient uptake and alkaline phosphatase (EC 3:1:3:1) activity of *Emiliania huxleyi* (prymnesiophyceae) during growth under N and P limitation in continuous cultures. *J. Phycol.*, **36**, 87–96.

Rousseau, V., Breton, E., De Wachter, B., Beji, A., Deconinck, M., Huijgh, J., Bolsens, T., Leroy, D. *et al.* (2004) Identification of Belgian maritime zones affected by eutrophication. In *Scientific Support Plan for a Sustainable Development Policy-Sustainable Management of the North Sea*. Belgian Science Policy Office (Belspo), Brussels.

Rousseau, V., Mathot, S. and Lancelot, C. (1990) Calculating carbon biomass of *Phaeocystis* sp. from microscopic observations. *Mar. Biol.*, **107**, 305–314.

Salihoglu, B., Garçon, V., Oschlies, A. and Lomas, M. W. (2007) Influence of nutrient utilization and remineralization stoichiometry on phytoplankton species and carbon export: a modeling study at BATS. *Deep Sea Res. Part I*, **55**, 73–107.

Shaked, Y., Xu, Y., Leblanc, K. and Morel, F. M. M. (2006) Zinc availability and alkaline phosphatase activity in *Emiliania huxleyi*: implications for Zn-P co-limitation in the ocean. *Limnol. Oceanogr.*, **51**, 299–309.

Sohm, J. A. and Capone, D. G. (2006) Phosphorus dynamics of the tropical and subtropical north Atlantic: *Trichodesmium* spp. versus bulk plankton. *Mar. Ecol. Prog. Ser.*, **317**, 21–28.

Sterner, R. W. and Elser, J. J. (2002) *Ecological Stoichiometry: The Biology of Elements from Molecules to the Biosphere*. Princeton University Press, Princeton, 439 p.

Taylor, K. E. (2001) Summarizing multiple aspects of model performance in a single diagram. *J. Geophys. Res.*, **106**, 7182–7192.

van Boekel, W. H. M. (1991) Ability of *Phaeocystis* sp. to grow on organic phosphates: direct measurement and prediction with the use of an inhibition constant. *J. Plankton Res.*, **13**, 959–970.

van Boekel, W. H. M. and Veldhuis, M. J. W. (1990) Regulation of alkaline phosphatase synthesis in *Phaeocystis* sp. *Mar. Ecol. Prog. Ser.*, **61**, 281–289.

van Der Zee, C. and Chou, L. (2005) Seasonal cycling of phosphorus in the Southern Bight of the North Sea. *Biogeosciences*, **2**, 27–42.

Veldhuis, M. J. W. and Admiraal, W. (1987) Influence of phosphate depletion on the growth and colony formation of *Phaeocystis pouchetii*. *Mar. Biol.*, **95**, 47–54.

Veldhuis, M. J. W., Colijn, F. and Admiraal, W. (1991) Phosphate utilization in *Phaeocystis pouchetii (Haptophyceae)*. *Mar. Ecol.*, **12**, 53–62.

Veldhuis, M. J. W., Venekamp, L. A. H. and Ietswaart, T. (1987) Availability of phosphorus sources for blooms of *Phaeocystis pouchetii (Haptophyceae)* in the North Sea: impact of the river Rhine. *Neth. J. Sea Res.*, **21**, 219–229.

Vidal, M., Duarte, C. M., Agustí, S., Gasol, J. M. and Vaqué, D. (2003) Alkaline phosphatase activities in the central Atlantic Ocean indicate large areas with phosphorus deficiency. *Mar. Ecol. Prog. Ser.*, **262**, 43–53.

Wagner, F., Sahan, E. and Falkner, G. (2000) The establishment of coherent phosphate uptake behaviour by the cyanobacterium *Anacystis nidulans*. *Eur. J. Phycol.*, **35**, 243–253.

Wurch, L. L., Bertrand, E. M., Saito, M. A., Van Mooy, B. A. S. and Dyhrman, S. T. (2011) Proteome changes driven by phosphorus deficiency and recovery in the brown tide-forming alga *Aureococcus anophagefferens*. *PLoS One*, **6**, e28949.

Xu, Y., Boucher, J. M. and Morel, F. M. M. (2010) Expression and diversity of alkaline phosphatase ehap1 in *Emiliania huxleyi* (Prymnesiophyceae). *J. Phycol.*, **46**, 85–92.

Xu, Y., Wahlund, T. M., Feng, L., Shaked, Y. and Morel, F. M. M. (2006) A novel alkaline phosphatase in the coccolithophore *Emiliania huxleyi* (prymnesiophyceae) and its regulation by phosphorus. *J. Phycol.*, **42**, 835–844.

Yamaguchi, H., Arisaka, H., Otsuka, N. and Tomaru, Y. (2014) Utilization of phosphate diesters by phosphodiesterase-producing marine diatoms. *J. Plankton Res.*, **36**, 281–285.